Supporting Information:

METHODS

AAV injection

Adapted from previous publications (1, 2):

1. The multicolor AAV mix was injected unilaterally (60 µl/mouse) into the retro-orbital sinus of male and female mice aged 7-10 weeks.
2. The master mix was vortexed for 1–2 s before use.
3. Mice were placed in the induction chamber in a fume hood and anesthetized initially with 4.5% isoflurane in oxygen and 2.5% during the injection.
4. The vectors were loaded without air bubbles in a BD Veo Insulin Syringe with BD Ultra-Fine 6 mm x 31G needle (324911, Becton, Dickinson and Company, Franklin Lakes, NJ).
5. The anesthetized mouse was removed from the induction chamber, and placed in a prone position with the nose cone to maintain anesthesia.
6. The needle was inserted, bevel down, at a 30–45° angle into the medial canthus and through the conjunctival membrane to the retro-orbital sinus.
7. The vectors were injected slowly into the retro-orbital sinus and the needle was removed gently.
8. Mice survived 3 weeks before tissue collection, which was the time AAV transduction reaches steady-state levels or robust labeling was reported using similar AAV-PHP.S and AAV9 vectors and doses in mice (2-4).

Tissue Preparation:

1. Mice were euthanized by an overdose of 5% isoflurane in oxygen.
2. After thoracotomy, perfusion cannula (18G) was inserted into the aorta via the left ventricle.
3. Saline was perfused for ~1 min.
4. The gastrointestinal (GI) tract from the lower esophagus to rectum was removed.
5. The whole colon from ileocecal junction to the end of distal colon at the level of pelvic brim where runs the iliac artery, as well as the lower esophagus, gastric corpus, gastric antrum, 1 cm of jejunum and 1 cm of ileum at 3-5 cm and 2-3 cm from the ileocecal junction respectively and rectum were flat-pinned on a Sylgard™ 184 silicone elastomer (Electron Microscopy Science, Hatfield, PA).
6. Perfusion of mouse with 40 ml of cold 4% paraformaldehyde in 0.1 phosphate buffer (pH 7.3) at 2 ml/min.
7. The pelvic, celiac and dorsal root (L6) ganglia were dissected out.
8. Post-fixation of the ganglia in 4% paraformaldehyde at 4°C overnight.
9. The GI tissues and ganglia were rinsed in 0.01 M phosphate-buffer saline (PBS) for 1 day.
10. ~~The~~ colon ~~of some mice was~~ prepared to maintain the layers from submucosa to serosa by scratching of the mucosa, because the mucosa ~~is~~ not cleared well when embedded in

Refractive Index Matching Solution (RIMS, recipe below), and it interferes with the focus of laser beams during image acquisition in the whole colon wall.

11. Tissues were cleared by immersion in a custom-made imaging media, RIMS (5) with a reflective index of 1.46~~]~~, 2 h at room temperature for ganglia and overnight at 4°C for GI tissues.
12. The ganglia after 2 h and GI tissues after overnight immersion in RIMS were embedded on microscopic glass slides in fresh RIMS sealed by iSpacer (SunJin Lab Co., Hsinchun City, Taiwan, www.sunjinlab.com). The colon samples were placed onto the slides with serosa on top.

Refractive Index Matching Solution (RIMS)

Histodenz (Sigma D2158)	40 g	88%
Tween-20	30 µl	0.1%
Sodium azide	3 mg	0.01%
0.02 M phosphate buffer (pH7.5)	30 ml	

Microscopy information: in ~~Supporting information name as "SI(2)_~~Table S1 ~~Photomicrography info"~~

Digital segmentation and neuronal tracing in confocal image

Software: Neurolucida (NL)360 (version 2020.1.1.), NL Explorer (version 2019.2.1.), Imaris 9.2 for Neuroscience and a customized version of neuTube (6).

Microscopic image post-processing: presented as original confocal microscopic images visualized in Imaris 9.2 with adjusted brightness, but no deconvolution, noise ratio cutoff and contrast adjusting. Images presented in the figures of the article had a 20% increase in brightness just for visual~~izing~~ effect.

Digital neuronal tracing: NL360 and Imaris 9.2: Adaptive thresholds were used in tracing algorithms, not isosurfacing, using semi-automated, namely user-guided mode (NL360), or manual tracing ~~or~~ filament (Imaris). Somas were detected by sensitivity based on contrast between foreground and background (NL360) or surface detection (Imaris). Nerve fibers were traced by points, without tortuosity limits. Wrong routes of traces in fiber-dense regions or fibers with similar hues were manually traced and corrected.

All the programs used in this study traced soma and neurites in separate modes in the confocal microscopic images. Varicosities were not spotted because none of the software we used had the ability. When the individual structures were traced, the original images were adjusted by whiteness and/or contrast to the detectable thresholds. For the white fluorescence ("hue bleaching") by intensive AAV labeling, tracing was performed in one or two colors instead of all channels. Whereas for faint elements, brightness/contrast was increased. Manual tracing was used when there was interfering by close-by labeling or the fluorescence was under automated detectable levels. The digital traces were confirmed by magnification, rotation, partial projection or dicer of layers. Axons were identified by varicosities or thin fiber with the same diameter.

The customized version of neuTube was used to trace a subset of samples. Weighted combinations of spectral channels were generated using a custom MATLAB script to highlight subsets of cells with specific relative expression of XFPs, which were traced in semi-automated fashion.

Images demonstrating conformation of neuronal contacts

Selected images demonstrate how the specific features were confirmed for digital tracing.

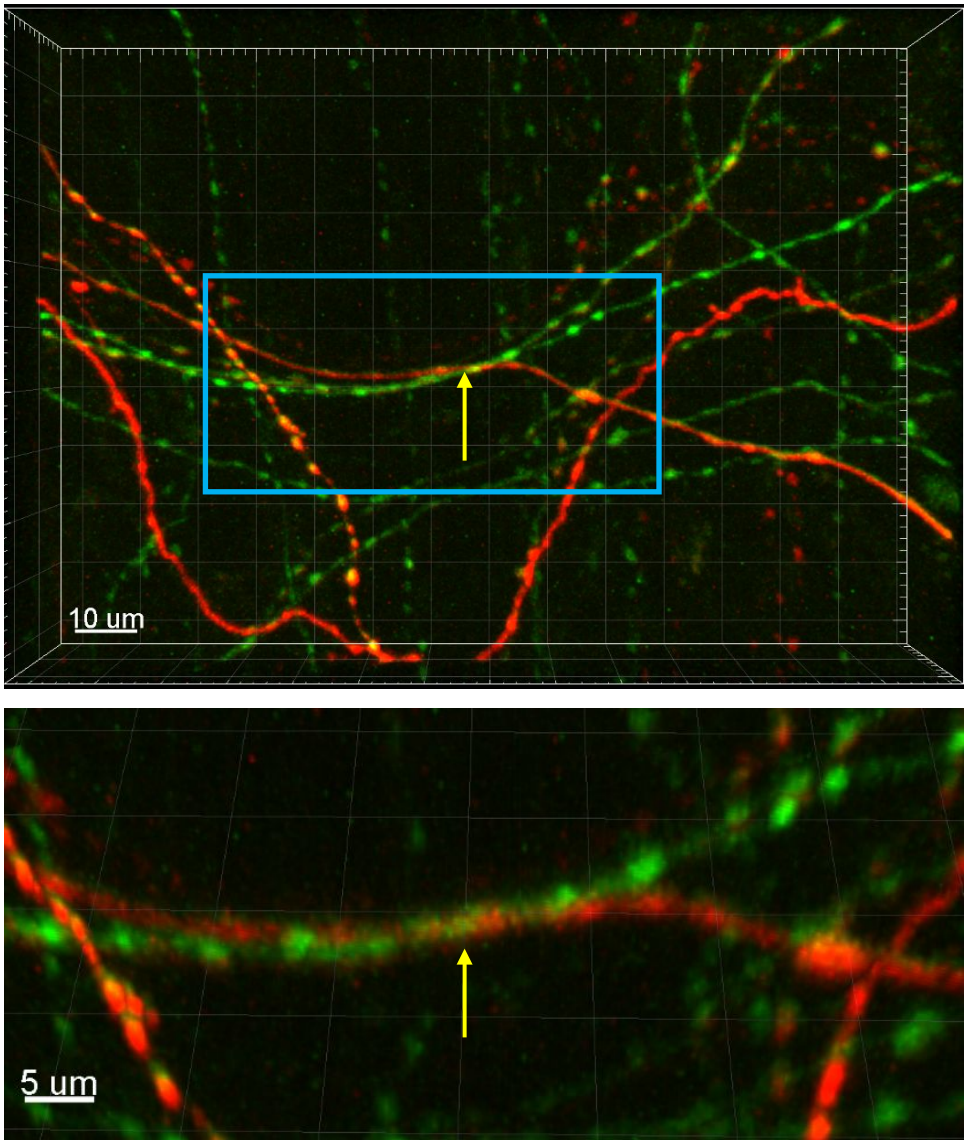

Parallel contacts of axon and passing fiber. Images 3D cropped in Imaris from Fig. 4A. Red and green channels were selected and brightness was adjusted. The parallel contacts (arrow indicated in Fig. 4A) of one axon of a neuron (white colored in Fig. 4B) and one passing fiber. The image in green channel can also be view in 3D in Video 3.

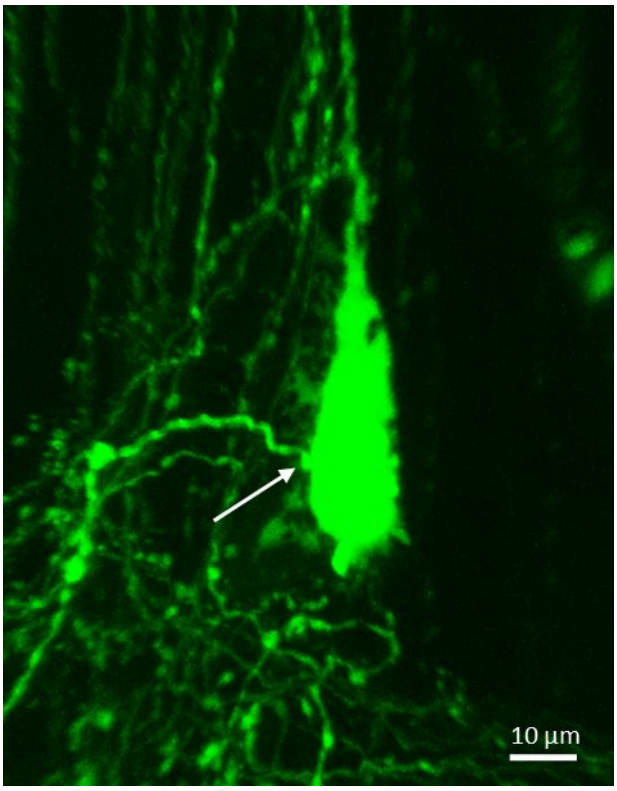

Left panel: Axon origin. The confocal image of Fig. 2A was 3D cropped, and turned about ~25° along the Y axis to the right using Imaris. Only the green channel was selected, in which brightness was adjusted. The arrow indicates the origin of one axon from neuron #5.

Lower Panel: Neuronal contacts. The confocal image of Fig. S4A was cropped in 3D and adjusted for brightness using Imaris. The red arrow indicates the one axon branch turned ~180°, and the orange arrows a nerve fiber that contacted neuronal soma, dendrites and axon *en route*, which are digitally traced in Fig. S4B using NL360.

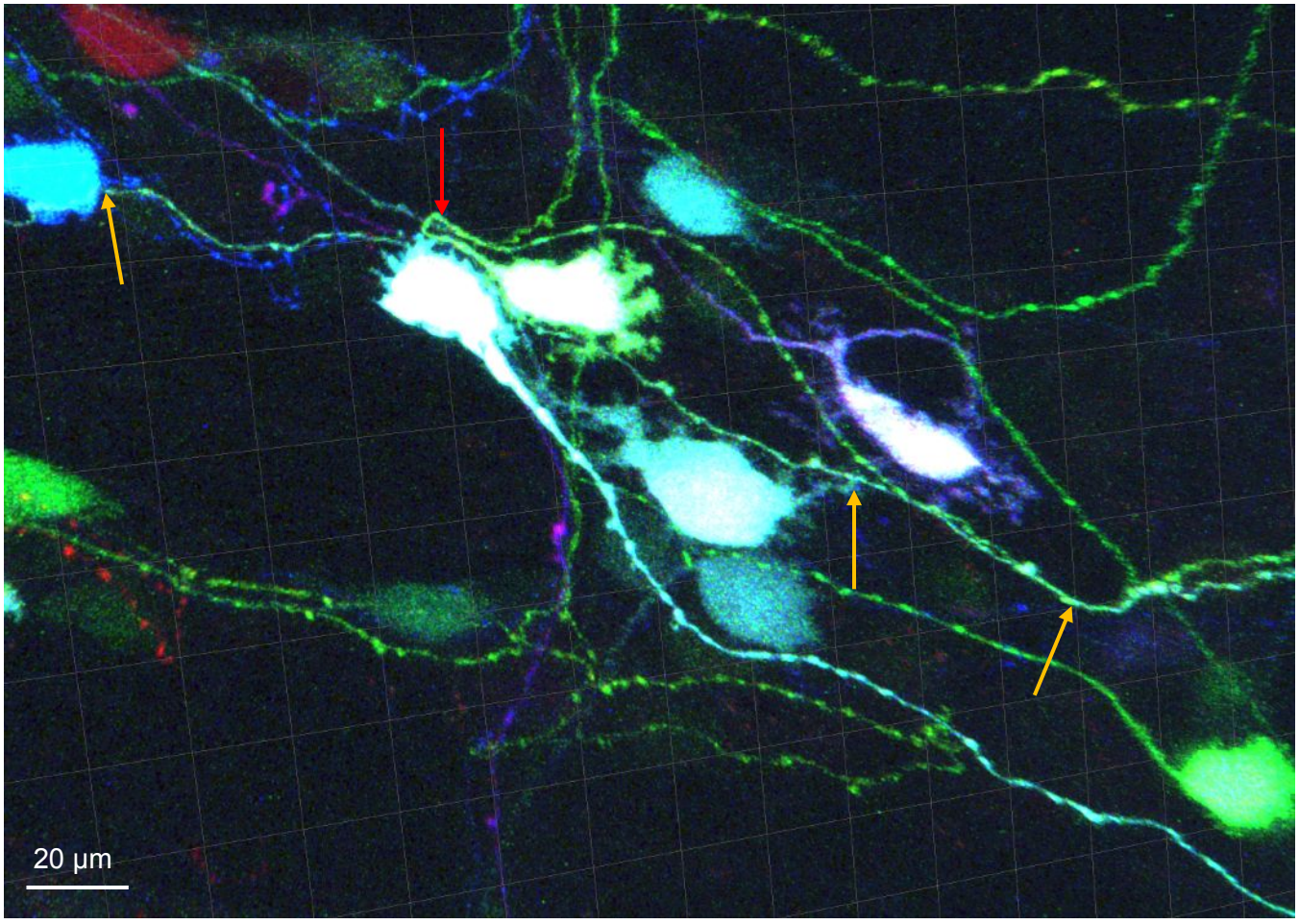

Soma measurements

Thirty confocal images of the AAV-XFP labeled proximal colon were selected from 4 male and 4 female mice injected iv with a multicolor 4-AAV vectors system (AAV-PHP.S:hSyn-tTA:TRE-XFP; inducer doses were $1x10^{10}$, $5x10^{10}$ and $1x10^{11}$ GC/mouse) 3 weeks before. The neuronal somas were digitally traced in 3D using semi-manual mode in NL360 with the sensitivity adjusted for each some based on contrast between foreground and background. The soma measurement was performed in NL Explorer in 3D, and the 2D parameters were collected from the largest area and grouped by size (area, major and minor diameters) and shape (ratio of major/minor diameter). Areas, diameters and ratio were measured in each contour that traced the soma shape in each optical section acquired in a confocal microscope. The size of the area is the largest one of each soma. The major diameter is the longest diameter in the largest area and the minor diameter is the one crossing the center of the major diameter in a right angle. The neuronal sizes as small, medium and large were determined by the largest area of <200, 200-400 and >400 μm^2, or major diameters of <20, 20-30 and >30 μm. The round, oval and elongated neurons were defined by the ratio of major/minor diameters <1.33, 1.3-2.5 and >2.5. We did not present 3D volume of the somas, because some of the somas were glaring due to fluorescent diffraction in the z-axis or partially cut when setting the Z-stacks in the confocal images.

References

1. Yardeni T, Eckhaus M, Morris HD, Huizing M, Hoogstraten-Miller S. Retro-orbital injections in mice. *Lab animal*. 2011;40(5):155-60.
2. Challis RC, Ravindra Kumar S, Chan KY, Challis C, Beadle K, Jang MJ, et al. Systemic AAV vectors for widespread and targeted gene delivery in rodents. *Nature protocols*. 2019;14(2):379-414.
3. Chan KY, Jang MJ, Yoo BB, Greenbaum A, Ravi N, Wu WL, et al. Engineered AAVs for efficient noninvasive gene delivery to the central and peripheral nervous systems. *Nat Neurosci*. 2017;20(8):1172-9.
4. Gombash SE, Cowley CJ, Fitzgerald JA, Hall JC, Mueller C, Christofi FL, et al. Intravenous AAV9 efficiently transduces myenteric neurons in neonate and juvenile mice. *Front Mol Neurosci*. 2014;7:81.
5. Yang B, Treweek JB, Kulkarni RP, Deverman BE, Chen CK, Lubeck E, et al. Single-cell phenotyping within transparent intact tissue through whole-body clearing. *Cell*. 2014;158(4):945-58.
6. Feng L, Zhao T, Kim J. neuTube 1.0: A New Design for Efficient Neuron Reconstruction Software Based on the SWC Format. *eNeuro*. 2015;2(1).

Table ~~1~~S: microcopy information

Figure #	Equipment	Software	Objective	Zoom	Fluorophores	Excitation	Emission Collection	Lasers	Master gain	Digital gain	Scaling	Image size
Fig 1A.	LSM 880, Axio Imager 2	Zen 2	Plan-Apochromat 10x/0.45 M27	Tiled 3x3	mTurquoise2 mNeonGreen mRuby2	458 488 555	465-486 517-553 586-624	4.0% 6.0% 4.0%	715 590 810	1.20 1.00 1.00	x: 0.83 µm y: 0.83 µm z: 2.80 µm	x: 2460 µm y: 2460 µm z: 190.4 µm
Fig 1B.	Zeiss Confocal LSM 710	Zen	Plan-Apochromat 20x/0.8 M27	0.8	mTurquoise2 mNeonGreen mRuby2	458 488 555	463-489 516-558 586-626	4.0% 6.0% 6.0%	667 810 819	1.00 1.00 1.00	x: 0.519 µm y: 0.519 µm z: 0.80 µm	x: 531.37 µm y: 531.37 µm z: 100.00 µm
Fig 1C.	Zeiss Confocal LSM 710	Zen	Plan-Apochromat 20x/0.8 M27	1	mTurquoise2 mNeonGreen mRuby2	458 488 555	463-489 516-558 586-626	4.0% 6.0% 5.0%	667 810 805	1.00 1.00 1.00	x: 0.692 µm y: 0.692µm z: 0.80 µm	x: 707.80 µm y: 707.80µm z: 82.40 µm
Fig. 1D	LSM 880, Axio Imager 2	Zen 2	Plan-Apochromat 20x/0.8 M27	1	mTurquoise2 mNeonGreen mRuby2	458 488 555	463-489 516-558 586-626	2.0% 1.1% 2.0%	836 591 756	1.24 1.13 1.55	x: 0.415 µm y: 0.415µm z: 0.500 µm	x: 425.10 µm y: 425.10 µm z: 56.50 µm
Fig. 2A	Zeiss Confocal LSM 710	Zen	Plan-Apochromat 20x, NA 0.8	1	mTurquoise2 mNeonGreen mRuby2	458 488 555	463-489 516-558 586-626	4.0% 6.0% 6.0%	828 829 671	1.00 1.00 1.00	x: 0.163 µm y: 0.163 µm z: 0.500 µm	x: 424.94 µm y: 424.93 µm z: 43.00 µm
4A	Zeiss Confocal LSM 710	Zen	Plan-Apochromat 20x/0.8 M27	1	mTurquoise2 mNeonGreen mRuby2	458 488 555	463 - 489 516 - 558 586 - 626	4.0% 4.5% 2.4%	750 800 780	1.00 1.00 1.00	x: 0.415 µm y: 0.415 µm z: 0.770 µm	x: 425.10 µm y: 425.10 µm z: 50.05 µm
Fig S1 Esophagus	Zeiss Confocal LSM 710	Zen	EC Plan-Neofluar 10x/0.30 M27	1	mTurquoise2 mNeonGreen mRuby2	458 488 555	463-489 516-558 586-626	4.0% 5.0% 4.0%	700 800 786	1.00 1.00 1.00	x: 0.830 µm y: 0.830µm z: 1.000 µm	x: 849.36 µm y: 849.36 µm z: 42.00 µm
Fig S1 Gastric corpus	Zeiss Confocal LSM 710	Zen	EC Plan-Neofluar 10x/0.30 M27	1	mTurquoise2 mNeonGreen mRuby2	458 488 555	463-489 516-558 586-626	4.0% 5.0% 4.0%	700 800 786	1.00 1.00 1.00	x: 0.830 µm y: 0.830µm z: 1.000 µm	x: 849.36 µm y: 849.36 µm z: 90.00 µm
Fig S1 Gastric antrum	Zeiss Confocal LSM 710	Zen	EC Plan-Neofluar 10x/0.30 M27	1	mTurquoise2 mNeonGreen mRuby2	458 488 555	463-489 516-558 586-626	4.0% 5.0% 4.0%	700 800 786	1.00 1.00 1.00	x: 0.830 µm y: 0.830µm z: 1.000 µm	x: 849.36 µm y: 849.36 µm z: 51.00 µm
Fig S1 Jejunum	Zeiss Confocal LSM 710	Zen	EC Plan-Neofluar 10x/0.30 M27	1	mTurquoise2 mNeonGreen mRuby2	458 488 555	463-489 516-558 586-626	4.0% 5.0% 4.0%	700 800 786	1.00 1.00 1.00	x: 0.830 µm y: 0.830µm z: 1.000 µm	x: 849.36 µm y: 849.36 µm z: 100.00 µm
Fig S1 Ileum	Zeiss Confocal LSM 710	Zen	EC Plan-Neofluar 10x/0.30 M27	1	mTurquoise2 mNeonGreen mRuby2	458 488 555	463-489 516-558 586-626	4.0% 5.0% 4.0%	700 800 786	1.00 1.00 1.00	x: 0.830 µm y: 0.830µm z: 1.000 µm	x: 849.36 µm y: 849.36 µm z: 150.00 µm
Fig S1 Proxomal colon	Zeiss Confocal LSM 710	Zen	EC Plan-Neofluar 10x/0.30 M27	1	mTurquoise2 mNeonGreen mRuby2	458 488 555	463-489 516-558 586-626	5.0% 5.0% 5.0%	667 800 780	1.00 1.00 1.00	x: 0.830 µm y: 0.830µm z: 1.000 µm	x: 849.36 µm y: 849.36 µm z: 99.00 µm
Fig S1 Transverse colon	Zeiss Confocal LSM 710	Zen	EC Plan-Neofluar 10x/0.30 M27	1	mTurquoise2 mNeonGreen mRuby2	458 488 555	463-489 516-558 586-626	4.0% 5.0% 4.0%	700 800 786	1.00 1.00 1.00	x: 0.830 µm y: 0.830µm z: 1.000 µm	x: 849.36 µm y: 849.36 µm z: 140.00 µm
Fig S1 Distal colon	Zeiss Confocal LSM 710	Zen	EC Plan-Neofluar 10x/0.30 M27	1	mTurquoise2 mNeonGreen mRuby2	458 488 555	463-489 516-558 586-626	4.0% 5.0% 4.0%	700 800 786	1.00 1.00 1.00	x: 0.830 µm y: 0.830µm z: 1.000 µm	x: 849.36 µm y: 849.36 µm z: 60.00 µm
Fig S1 Rectum	Zeiss Confocal LSM 710	Zen	EC Plan-Neofluar 10x/0.30 M27	1	mTurquoise2 mNeonGreen mRuby2	458 488 555	463-489 516-558 586-626	4.0% 5.0% 4.0%	630 800 810	1.00 1.00 1.00	x: 0.830 µm y: 0.830µm z: 1.000 µm	x: 849.36 µm y: 849.36 µm z: 166.00 µm
Fig. S2. DRG	Zeiss Confocal LSM 710	Zen	EC Plan Neofluar 10x/0.30 M27	0.8	mTurquoise2 mNeonGreen mRuby2	458 488 555	463-489 516-558 586-626	4.5% 6.0% 4.0%	825 851 726	1.23 1.23 1.23	x: 1.038 µm y: 1.038 µm z: 1.000 µm	x: 1061.70 µm y: 1061.70 µm z: 198.00 µm
Fig. S2. Celiac	Zeiss Confocal LSM 710	Zen	EC Plan Neofluar 10x/0.30 M27	0.6	mTurquoise2 mNeonGreen mRuby2	458 488 555	463-489 516-558 586-626	4.5% 8.0% 4.0%	825 851 726	1.23 1.23 1.00	x: 1.384 µm y: 1.384 µm z: 1.384 µm	x: 1024 µm y: 1024 µm z: 345 µm
Fig S2. Pelvic	Zeiss Confocal LSM 710	Zen	EC Plan Neofluar 10x/0.30 M27	1	mTurquoise2 mNeonGreen mRuby2	458 488 555	463-489 516-558 586-626	6.0% 6.0% 4.0%	630 800 810	1.00 1.00 1.00	x: 0.830 µm y: 0.830 µm z: 1.000 µm	x: 850.19 µm y: 850.19 µm z: 174.00 µm
Fig S4A	Zeiss Confocal LSM 710	Zen	Plan-Apochromat 20x/0.8 M27	0.8	mTurquoise2 mNeonGreen mRuby2	458 488 555	463-489 516-558 586-626	6.0% 6.0% 6.0%	891 829 762	1.23 1.00 1.21	x: 0.519 µm y: 0.519 µm z: 0.770 µm	x: 530.85 µm y: 530.85µm z: 33.12 µm
Fig S5A.	Zeiss Confocal LSM 710	Zen	Plan-Apochromat 20x/0.8 M27	1	mTurquoise2 mNeonGreen mRuby2	458 488 555	463-489 516-558 586-626	4.0% 3.0% 3.0%	650 770 780	1.00 1.00 1.00	x: 0.415 µm y: 0.415 µm z: 1.000 µm	x: 425.10 µm y: 425.10 µm z: 96.00 µm
Fig. S6A	Zeiss Confocal LSM 710	Zen	Plan-Apochromat 20x/0.8 M27	0.6	mTurquoise2 mNeonGreen mRuby2	458 488 555	463-489 516-558 586-626	6.0% 6.0% 4.0%	667 810 800	1.00 1.00 1.00	x: 0.692 µm y: 0.692 µm z: 1.000 µm	x: 708.49 µm y: 708.49 µm z: 160.00 µm
Fig. S6A	Zeiss Confocal LSM 710	Zen	Plan-Apochromat 20x, NA 0.8	0.8	mTurquoise2 mNeonGreen mRuby2	458 488 555	463-489 516-558 586-626	5.0% 7.0% 6.0%	793 821 733	1.23 1.04 1.21	x: 0.692 µm y: 0.692 µm z: 0.200 µm	x: 707.92 µm y: 707.80 µm z: 32.00 µm
Fig S7A	Zeiss Confocal LSM 710	Zen	Plan-Apochromat 20x/0.8 M27	0.8	mTurquoise2 mNeonGreen mRuby2	458 488 555	463-489 516-558 586-626	6.0% 6.0% 4.0%	667 810 819	1.00 1.00 1.00	x: 0.519 µm y: 0.519 µm z: 0.800 µm	x: 531.37 µm y: 531.37 µm z: 100.00 µm
Fig S8A	Zeiss LSM 880, Axio Imager 2	Zen 2	Plan-Apochromat 10x/0.45 M27	Tiled 3x3	mTurquoise2 mNeonGreen mRuby2	458 488 555	465-486 517-553 586-624	6.5% 2.2% 3.0%	715 590 810	1.00 1.00 1.00	x: 0.692 µm y: 0.692 µm z: 1.000 µm	x: 708.49 µm y: 708.49 µm z: 50.00 µm
Fig S8B	Zeiss Confocal LSM 710	Zen	Plan-Apochromat 20x/0.8 M27	1	mTurquoise2 mNeonGreen mRuby2	458 488 555	463-489 516-558 586-626	4.0% 6.0% 5.5%	700 809 790	1.00 1.00 1.00	x: 0.692 µm y: 0.692 µm z: 1.000 µm	x: 708.49 µm y: 708.49 µm z: 120.00 µm
Fig S8C	Zeiss Confocal LSM 710	Zen	Plan-Apochromat 20x/0.8 M27	1	mTurquoise2 mNeonGreen mRuby2	458 488 555	463-489 516-558 586-626	4.0% 5.0% 4.0%	700 780 735	1.00 1.00 1.00	x: 0.519 µm y: 0.519 µm z: 0.900 µm	x: 531.37 µm y: 531.37 µm z: 83.70 µm

Video captions

Video 1. A video created in Imaris demonstrating the multicolor AAV labeled neurons and fibers in myenteric, circular muscles and submucosal layers of proximal colon. The myenteric plexus contains better labeling than submucosal plexus. The image was obtained from a female mouse injected retro-orbitally with a multicolor 4-AAV vectors (AAV-PHP.S:hSyn-tTA:TRE-XFP) and inducer dose was $1x10^{11}$ GC/mouse). The myenteric plexus layer is in the front of the image with well-labeled neuronal somas and fibers. The nerve fibers in the circular muscle layer are "beneath" the myenteric plexus, running vertically. The neurons in the submucosal plexus were displayed as multiple colored somas in the back layer.

Video 2. A video created in Imaris demonstrating a complex type of intraganglionic nerve endings in 3D view. The image was from the same mouse as in Video 1.

Video 3. A video created in Imaris demonstrating parallel contacts (arrow indicated in Fig. 4A) of one axon of a neuron (white colored in Fig. 4B) and one passing fiber.